Available online at www.sciencedirect.com
SCIENCE DIRECT®
International Journal of Heat and Fluid Flow 24 (2003) 284–298
International Journal of HEAT AND FLUID FLOW
www.elsevier.com/locate/ijhff

Size effect on single-phase channel flow and heat transfer at microscale

Zeng-Yuan Guo *, Zhi-Xin Li *

Department of Engineering Mechanics, Education Ministry Key Lab of Heat Transfer Enhancement and Energy Conservation, Tsinghua University, Beijing 100084, China

Abstract

The size effects on microscale single-phase fluid flow and heat transfer are reviewed and discussed. The physical mechanisms for the size effects on the microchannel flow and heat transfer were divided into two classifications: (a) The gas rarefaction effect occurs when the continuum assumption breaks down as the characteristic length of the flow becomes comparable to the mean free path of the molecules; (b) Variations of the predominant factors influence the relative importance of various phenomena on the flow and heat transfer as the characteristic length decreases, even if the continuum assumption is still valid. Due to the larger surface to volume ratio for microchannels, factors related to surface area have more impact to the microscale flow and heat transfer. Among them are: The surface friction induced flow compressibility in microchannels makes the fluid velocity profiles flatter and leads to higher friction factors and Nusselt numbers; The surface roughness of the microchannel is likely responsible for the early transition from laminar to turbulent flow and the increased friction factor and Nusselt number; The importance of viscous force in natural convection modifies the correlation between *Nu* and *Ra* for natural convection in a microenclosure and, other effects, such as the axial heat conduction in the channel wall, the channel surface geometry, and measurement errors as well, could lead to different flow and heat transfer behaviors from that at conventional scales.

Keywords: Microscale; Channel flow and heat transfer; Size effect; Single phase

1. Introduction

Nowadays microelectromechanical systems (MEMS) and micrototal analysis systems (μ-TAS) are having an important impact in medicine and bioengineering, information technologies and other industries, so their research is wide spread, especially basic and applied research on fluid flow and heat transfer at microscales. Some analytical and experimental results for the flow and heat transfer characteristics in microchannels are remarkably different from those for conventional-size channels, such as the variation of the friction factor, the heat transfer coefficient and the early transition from laminar to turbulent flow. Large differences exist in the reported friction factor ($0.5 < f/f_{conv} < 3.5$) and the heat transfer coefficients ($0.21 < Nu/Nu_{conv} < 16$) for single-phase flow through channels with hydraulic diameters ranging from 0.96 μm to 2.6 mm and in the reported Reynolds numbers ($300 < Re_c < 2300$) for transition from laminar to turbulent flow in microscale channels. For example, Wu and Little (1983) measured the friction factors for gas flow in very fine channels used for refrigerators. In their experiments, nitrogen, argon and hydrogen were used as working fluids with hydraulic diameters ranging from 45.46 to 83.08 μm, and *Re* varying from 100 to 15,000. The product of the friction factor and the Reynolds number (*fRe*) was as large as 118, which is much larger than the value of 64 for the laminar flow in conventional channels. Pfahler et al. (1990a, 1991) conducted a series of experimental studies with gases (N_2, He) and liquids (isopropyl and silicone oil) measuring the friction factor in microchannels with hydraulic diameters of 0.98–39.7 μm and *Re* ranging from 0.01 to 80. The measured friction factors were consistently lower than the theoretical predictions. Furthermore, the friction factor decreased with

* Corresponding authors. Tel.: +86-10-6278-2660; fax: +86-10-6278-1610 (Z.-Y. Guo), Tel.: +86-10-62772919; fax: 86-10-6278-1610 (Z.-X. Li).

E-mail addresses: demgzy@tsinghua.edu.cn (Z.-Y. Guo), lizhx@tsinghua.edu.cn (Z.-X. Li).

0142-727X/03/$ - see front matter © 2003 Elsevier Science Inc. All rights reserved.
doi:10.1016/S0142-727X(03)00019-5

Nomenclature

a	thermal diffusivity (m^2/s)
Bi	Biot number
c_p	specific heat (J/kg K)
C	friction constant
D, d	tube diameter (m)
D_h	hydraulic diameter (m)
Ec	Eckert number
f	friction factor
g	gravitational acceleration (m/s^2)
Gr	Grashof number
h	heat transfer coefficient (W/m^2 K)
k	ratio of specific heat
k_f	thermal conductivity of the fluid (W/m K)
k_s	thermal conductivity of the channel wall (W/m K)
Kn	Knudsen number
l	length (m)
L	tube length (m)
M	Mach number
M_{loc}	local Mach number
M_0	inlet Mach number
Nu	Nusselt number
p	Pressure (Pa)
p_b	back pressure (Pa)
p_0	entrance pressure (Pa)
P^*	dimensionless pressure
Pr	Prandtl number
r	radial coordinate (m)
R	radius (m)
Re	Reynolds number
T	temperature (K)
T_1	entrance temperature (K)
T_2	outlet temperature (K)
T_s	surface temperature (K)
u	axial velocity (m/s)
$\bar{u}$	velocity component related to incompressible flow (m/s)
$\hat{u}$	velocity component resulted from compressibility effect (m/s)
u_m	mean velocity (m/s)
u^*	dimensionless axial velocity
U	overall heat transfer coefficient (W/m^2 K)
x	axial coordinate (m)
X	dimensionless axial coordinate
Greeks	
μ	dynamic viscosity (kg/m s)
ν	kinetic viscosity (m^2/s)
ε	ratio of inertial force to viscous force
ε_τ	characteristic time ratio of diffusion and acceleration
ρ	density (kg/m^3)
ρ^*	dimensionless density
θ	dimensionless temperature
τ_a	characteristic time of gas acceleration (s)
τ_μ	characteristic time of diffusion (s)

decreasing Reynolds number for laminar flows when Reynolds number is small. Choi et al. (1991) measured the friction factors for nitrogen gas flow in microtubes for both the laminar and turbulent regimes. For Reynolds numbers smaller than about 400, the friction factor correlation had a value for the constant $C = fRe = 53$, instead of 64. Papautsky et al. (1999a,b) conducted experiments for water flow with hydraulic diameters ranging from 28.57 to 57.14 μm and Re ranging from 0.001 to 20. The normalized friction coefficient C for the experimental data was found to be approximately 1.12 for large Re and 1.2 for small Re. They concluded that the effect of the micropolar fluid, microscale effects at low aspect ratios, and the low Re were responsible for the high friction coefficients although it was not clear which was the dominant factor. Wang and Peng (1994) reported single-phase heat transfer coefficients in six rectangular channels having $0.31 < D_h < 0.75$ mm for water and methanol. Their Nusselt numbers were only 35% of those predicted by the Dittus–Boetler equation. However, Webb and Zhang (1998) found that their experimental results were adequately predicted by the commonly accepted correlations for single-phase flow in multiple tubes having hydraulic diameters between 0.96 and 2.1 mm. Johan et al. (2001) conducted measurements of the flow rate through silicon microchannels with a height of less than 0.9 μm and showed that standard macroscopic assumptions are still valid for laminar Newtonian fluids (silicon oil, ethanol) at flow rates as low as 0.2 nl/s. However, experiments with aqueous solution indicated anomalies in the form of low flow rates and time dependent variation. Wu and Little (1984) measured the flow and heat transfer characteristics for the flow of nitrogen gas in heat exchangers. Their Nusselt numbers for laminar flow ($Re < 600$) were lower than those predicted by standard correlations. For $600 < Re < 1000$ Nu was higher than the standard values. The laminar to turbulent heat transfer transition zone occurred at Re ranging from 1000 to 3000. Mala and Li (1999) measured the pressure drop and the flow rate for the flow of deionized water through microscale channels with diameters ranging from 50 to 254 μm. The measured pressure gradient was much higher than the standard

values. They correlated the measured pressure gradient as a function of Re and found that the transition flow regime started at $Re = 650$.

2. Size effect mechanism

New questions have arisen in microscale flow and heat transfer. For example, the causes for the large differences existing in the reported friction factors and heat transfer coefficients and their physical mechanisms are still unexplained. These problems have been discussed in several review papers by Gad-ed-Hak (1999), Mehendale et al. (1999), Drain et al. (1995) and Palm (2001). It is commonly recognized that gas rarefaction leads to lower friction factors and Nusselt numbers for microscale gas flows. The review by Gad-ed-Hak (1999) focused on the physics related to the breakdown of the N–S equations. Besides the rarefaction effect, Mehendale et al. (1999) noted that differences in the channel surface roughness could explain the disparities in the friction factors and the heat transfer data in some studies. They also thought that since the heat transfer coefficients were based on the inlet and/or outlet fluid temperatures, not the bulk temperature in almost all studies, comparison of conventional correlations is problematic. For the early transition from laminar to turbulent flow in microscale tubes, they pointed out that the thermophysical properties of the liquid change markedly as the fluid flows along the channel so that Re at the channel exit could be twice that at the inlet. Therefore, the early transition to turbulence might be partially attributed to the variation in Re. Drain et al. (1995) noted several effects that are improperly neglected when considering macroscale flow. For example, microscale phenomena may include two- or three-dimensional transport effects. Another observed microscale effect is the temperature dependent variations of the transport fluid properties along a microchannel which may invalidate the often used assumption of constant properties. They also suggested that improved measurement accuracies are required to provide conclusive evidence of microscale effects. Palm (2001) also suggested several possible explanations for the variations of microscale single-phase flow and heat transfer from conventional theory, including surface roughness effects, entrance effects, electric double-layer effects, non-constant fluid properties, two- and three-dimensional transport effects and the measurement accuracies. Guo (2000) classified the various mechanisms for the departure of flow and heat transfer correlations for flow in microchannels from the standard ones into two groups. First, if the characteristic length of the flow is on the same order of the magnitude as the molecular mean free path, the Navier–Stokes equations and the Fourier heat conduction equation break down and, consequently, the flow and heat transfer behaviors change considerably. This is the so-called rarefaction effect which can be represented by the Knudsen number, Kn (defined as the ratio of the molecular mean free path and the characteristic length of the flow). Secondly, the size effect on the flow and heat transfer correlations is attributed to the variation of the dominant factors or phenomena in the flow and heat transfer as the scale decreases even though the continuum assumption is still applicable. There may be various factors (for instance, boundary conditions or forces exerted on the fluid etc.) which affect the flow and heat transfer whose effect on the convection changes at different scales. Some phenomena (for instance, axial heat conduction in the tube wall), which are commonly neglected for normal-sized devices, may become important at microscale. As a result, microscale flow and heat transfer correlations must differ from those for normal-size devices. Karniadakis and Beskok (2002) addressed microflows with some emphases on the gas flow, where the main difference between fluid mechanics at microscales and in the macro domain can be broadly classified into four areas: non-continuum effects, low Reynolds number effects, surface-dominated effects, and multi-scales and multi-physics effects.

The assumption that the flow is a continuum is usually applicable for flow in MEMS with hydraulic diameters more than 1 μm ($Kn \sim 0.01$) to less than 1 mm ($Kn \sim 0.0001$). This is because even for the slip flow regime ($0.001 < Kn < 0.1$) the Navier–Stokes equation is still applicable as long as the slip boundary conditions are introduced to replace the non-slip boundary conditions. Therefore, gas rarefaction can be neglected and the macroscopic transport equations based on the continuum assumption are still valid. Therefore, the present discussion will focus on the size effect induced by the variation of dominant factors and phenomena in the flow and heat transfer as the device scale decreases, that is, the discussion will be limited to low Kn number.

Since the size effect due to the variation of dominant factors on the flow and heat transfer can be largely attributed to a very large surface to volume ratio for the microdevices, factors related to surface area will become more important as the device size decreases. Some relevant phenomena are the surface friction induced compressibility, the surface roughness, the predominant viscous forces and the surface geometry etc.

2.1. Surface friction induced flow compressibility

Gas flow in normal-sized tubes is usually assumed to be incompressible when the Mach number of flow in the channel is much less than unity, so the gas density can be regarded as constant along the channel. As the well-known fact, the flow in channels becomes fully developed and the product of the friction factor and Reynolds number is equal to a constant if the tube

length to diameter ratio is very large. For flow in microtubes, there are only several theoretical studies dealing with the effect of the compressibility on the gas flow and the heat transfer. Van der Berg et al. (1993a,b) solved the isothermal, compressible Navier–Stokes equations for laminar flow in a circular tube. For low Reynolds number and Mach number flows, they obtained a local "self-similar" velocity profile with the product *fRe* still equal to 64. Beskok et al. (1996) numerically modeled the competing effects of compressibility and rarefaction in internal flows in long channels. For shear-driven flows, the rarefaction dominated the momentum and energy transport, and the compressibility was negligible. Harley et al. (1995) conducted an experimental and theoretical investigation of subsonic, compressible flow in microsize, long conduits. They developed a one-dimensional model to evaluate the friction factor based on the locally fully developed approximation. Then, they solved the two-dimensional Navier–Stokes and energy equations for compressible flow of a gas between two isothermal, parallel plates for comparison. They concluded that the locally fully developed approximation could be used to interpret the experimental data for low and moderate Mach number flow. However, Guo and Wu (1997, 1998) found that the gas density variation along the microscale channel may be very large as the surface friction induced pressure drop per channel length is much larger than that for conventional-size channels. Numerical solution of the governing equations for compressible flow in a circular tube gave the pressure and density variations along the tube for isothermal flow at different inlet Mach numbers shown in Fig. 1 ($p_b/p_0 = \rho_b/\rho_0$ for the isothermal flow). The pressure variations may be large even for an inlet Mach number of 0.087 because the compressibility-induced gas acceleration and the increased momentum also contributed to the pressure decrease in addition to the friction. For compressible tube flow, the gas acceleration leads to the velocity profile changes not only in magnitude, but also in shape as shown in Fig. 2 (Guo and Wu, 1998). This is

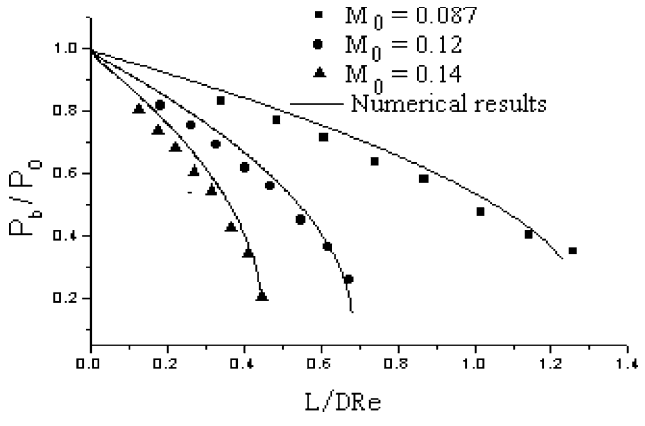

Fig. 1. Pressure and density variations along the flow direction.

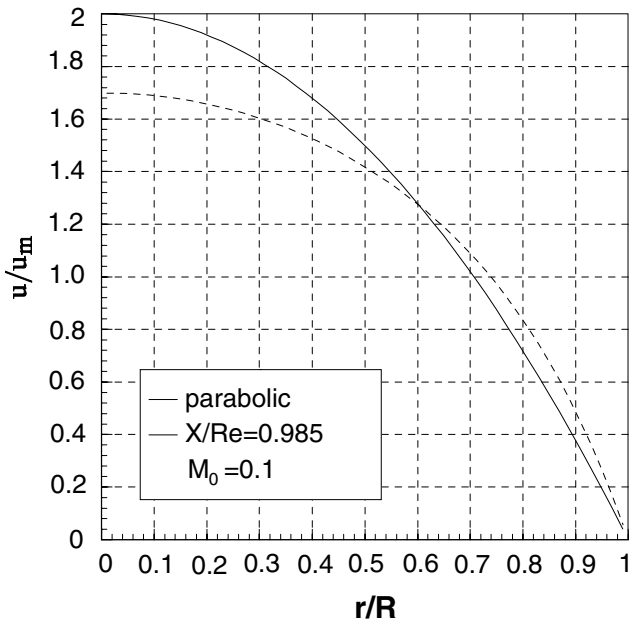

Fig. 2. Compressibility effect on the velocity profile.

because the velocity profile is dependent on two factors for compressible channel flows: the axial gas acceleration and radial viscous diffusion of momentum, which can be characterized by their characteristic times

$$\tau_a = \frac{1}{\frac{du_m}{dx}} \quad \text{and} \quad \tau_\mu = d^2/v \tag{1}$$

where u_m is the mean cross-sectional velocity of the gas flow. For a polytropic process, the ratio of the characteristic times of diffusion and acceleration, ε_τ, can be approximated as

$$\varepsilon_\tau = \tau_\mu/\tau_a = 8kM^2(x) \tag{2}$$

which represents the relative importance of diffusion and acceleration. Eq. (2) shows that the time ratio is a function of Mach number only. When $M(x) \ll 1$, $\varepsilon_\tau \ll 1$, that is the viscous diffusion process is much faster than the acceleration process, then the velocity profile remains parabolic as for incompressible flow in a circular tube. $\tau_\mu \gg \tau_a$ implies that the acceleration process dominates as long as the Mach number of the subsonic flow is not far from unity. As a result, the velocity profiles become flatter as the gas flow downstream, much flatter than a parabolic distribution, as shown in Fig. 2. Thus, in microscale channels, fully developed or locally fully developed gas flow impossibly occur even for channels with very large length to diameter ratio. The magnitude increments produce additional pressure drop, while the shape changes alter the friction factor correlation from its conventional correlation. The numerical results for the compressibility effect on the friction coefficients are illustrated in Fig. 3 (Guo and Wu, 1998).

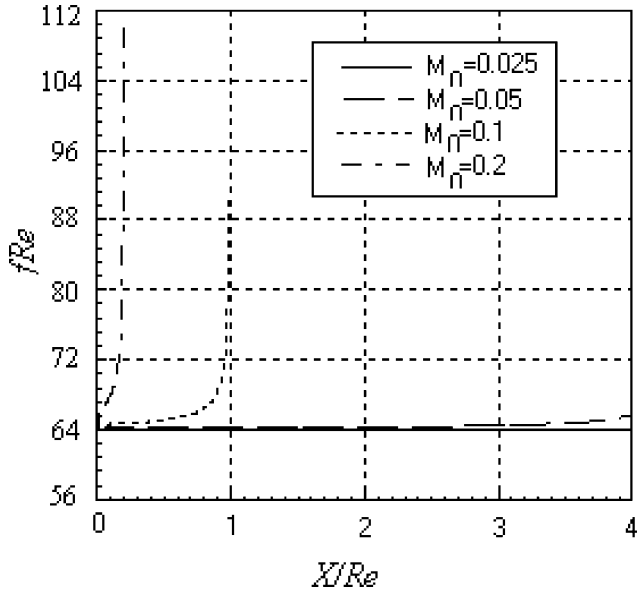

Fig. 3. Dependence of *fRe* on location for various inlet Mach numbers.

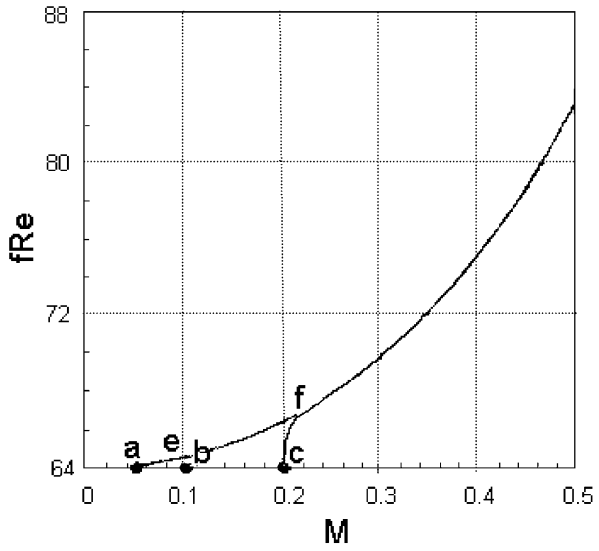

Fig. 4. Friction factor variation for various local Mach numbers (Guo and Wu, 1998).

Li et al. (1999) analytically studied the compressibility effect on gas flow in microtubes. Assuming that the Mach number is not close to unity, the velocity, u, can then be divided into two parts, $u = \bar{u} + \hat{u}$, where $\bar{u}$ is parabolic and $\hat{u}$ is the velocity component resulting from the flow compressibility. Their non-dimensional momentum equations were solved analytically to give the approximate correlations for the velocity and friction factor

$$u^* = M_0^{-2/(n+1)} M^{2/(n+1)} \left[2\left(1 - r^{*2}\right) + \frac{2}{n+1} M^{-1} M_{x^*} \left(\frac{r^{*2}}{2} - \frac{r^{*4}}{2} + \frac{r^{*6}}{9} - \frac{1}{9} \right) \right] \tag{3}$$

$$f = \frac{64}{Re} + \frac{64}{Re} \frac{M^2}{1.5 - 0.66M - 1.14M^2} \tag{4}$$

The result in Eq. (3) shows that the deviation of the velocity profile of gas flow in a microtube from parabolic depends on the Mach number. Eq. (4) clearly indicates that the friction factor is not only a function of *Re*, but is also a function of the Mach number.

The numerical results of Guo and Wu (1998) also showed that the product of the local friction factor, f, and *Re* was not a constant, but was a function of the local Mach number, as shown in Fig. 4. Therefore, neglecting the effect of the flow compressibility on the friction factor and the Nusselt number may be one major reason for the discrepancies between experimental and analytical results for gas flow and heat transfer in microtubes reported by different investigators.

Li et al. (2000a) employed a tube-cutting method to measure the local pressures and local Mach numbers along a microtube. The experimental data and numerical results are shown in Figs. 1 and 5. The results again show that for flow in microtubes, the pressure variations are significant along the tube, and the local Mach number of the gas flow increases with increasing dimensionless distance from the inlet, and may become very large even for the small inlet Mach numbers. This phenomenon is critical for the design of microsystems since choking ($M = 1$ at channel outlet) may occur in channel flows even for cases where the inlet Mach number is much smaller than unity. The characteristics of flow in microdevices was found to change from a cubic dependence to a linear dependence on the channel diameter for sonic flow in the channel, as mentioned by Jerman's work dealing with micromachined diaphragm valves (Jerman, 1990).

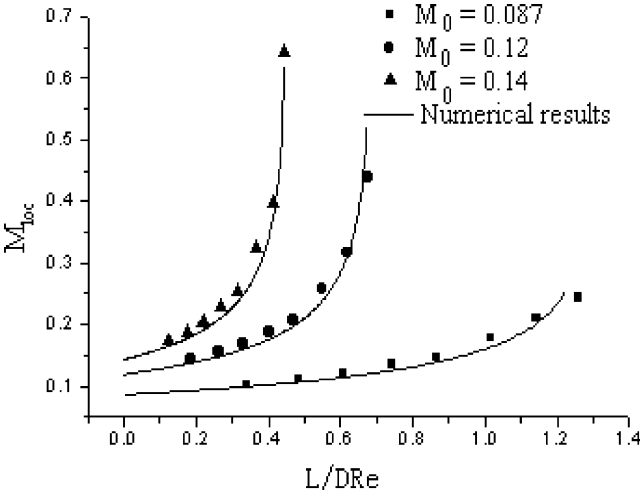

Fig. 5. Local Mach number variation along a microtube (Li et al., 2000a,b).

The radial temperature profiles in the fluid are strongly dependent on the radial velocity profiles for tube flows. As above-mentioned, the gas flow in microscale channels is impossibly fully developed or locally fully developed. Therefore, no fully developed temperature profiles will occur as long as the flow is developing. In addition, numerical results presented by Du (2000) showed that the local Eckert numbers, like the friction factors, increase along the flow direction. Furthermore, in view of the compressibility induced increase of Mach number, the Eckert number of the downstream flow may be rather large, even though the inlet Eckert number is small, as shown in Fig. 6. As a consequence, the viscous dissipation and the work due to expansion can not be neglected in these cases. The work due to expansion leads to a gas temperature decrease in the channel interior, while the viscous dissipation results in a gas temperature rise in the near-wall region, shown in Fig. 7. The fluid temperature profiles are quite different with and without the *Ec* effects. The temperature rise in the near-wall region leads to increased heat transfer. It should be noted that the conventionally defined Nusselt number may even be negative, as shown in Fig. 8, if the Mach number and the resulting consequent temperature decrease in the channel interior are large enough. A negative Nusselt number is physically meaningless, which can be attributed to the inappropriate definition of the characteristic temperature difference. The adiabatic temperature difference, instead of the difference between the wall temperature and the bulk fluid temperature, should be taken as the characteristic temperature difference to describe the channel heat transfer in the high speed flow.

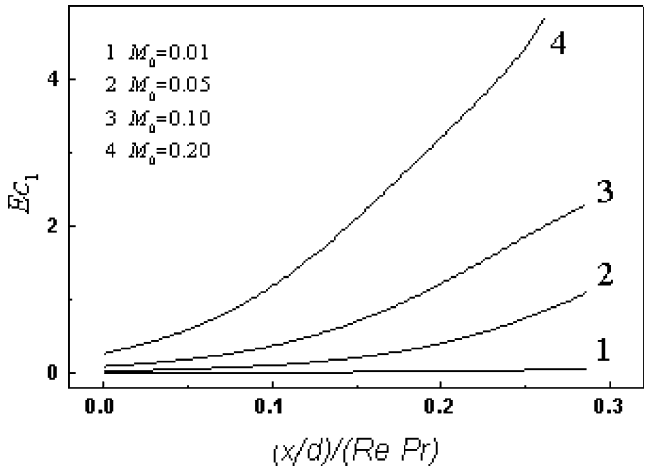

Fig. 6. Variation of Eckert number along the tube (Du, 2000).

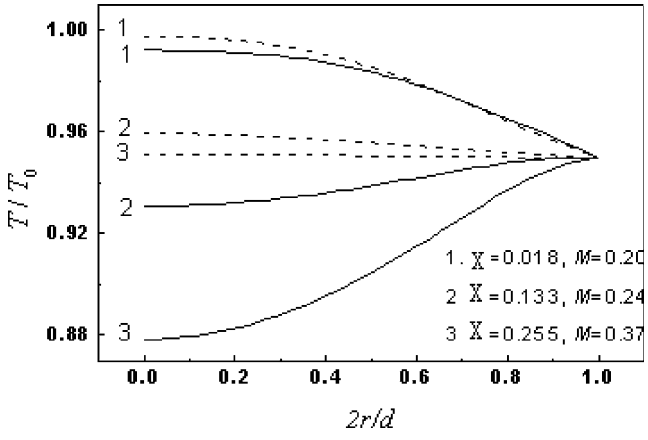

Fig. 7. Temperature profiles with and without *Ec* effect: — with *Ec* effect; - - - without *Ec* effect.

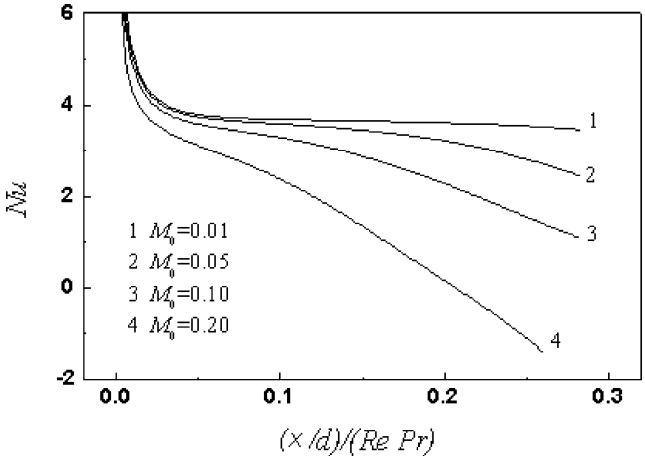

Fig. 8. Variation of Nusselt number along the tube.

2.2. Surface roughness

Only a few studies have considered the effect of roughness on laminar flow since Nikuradse (1933) and Moody (1944) concluded more than half a century ago that if internal relative wall roughness is less than 5%, the roughness effect on the laminar flow characteristics can be ignored. Numerous studies between 1932 and 1944 (Drew et al., 1932; Kemler, 1933; Pigott, 1933) on laminar flow in circular tubes showed that the theoretical estimate of the magnitude of the maximum roughness size, which will not alter the velocity profile in pipes, was still quite small relative to pipe sizes available at that time. Nevertheless, some experimental and computational results for laminar flows have also contradicted the Moody's well-known conclusion. Nikuradse's conclusion still pervades today because the flow in conventional-sized coarse tubes is usually turbulent, so laminar flows are of less practical importance. However, flows in microchannels are often laminar, so the study of laminar flow in rough microchannels has become important.

The study of the roughness effect on the flow characteristics in microchannels is very difficult, because

there are a large number of parameters describing the various roughness geometries. The equivalent sand roughness defined by Nikuradse has been used successfully in practical designs. However, no similar works have been found dealing with the effect of roughness on laminar incompressible fluid flow in channels.

The effect of channel size on the flow behavior was studied experimentally using water flow in smooth glass and silicon microchannels with diameters ranging from 80 to 166 μm (Guo, 2000). The results given in Fig. 9 show that the flow behavior is very similar to that for normal-sized channels, with the product of the Darcy friction factor and the Reynolds number, *fRe*, approximately a constant of 64 and the transition from laminar to turbulent flow beginning at around $Re = 2100$–2300.

Experimental data for the friction factor for gas flow in smooth microchannels are shown in Fig. 10. Again, the friction factors are close to the standard value as long as the Mach number is less than 0.3, beyond that

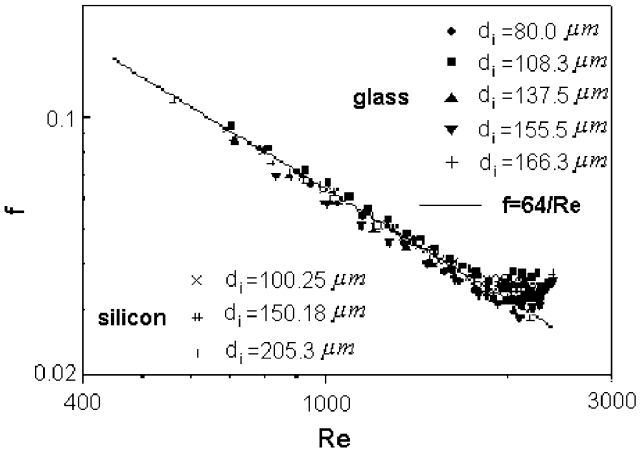

Fig. 9. Friction factor for water flow in smooth microtubes (Guo, 2000).

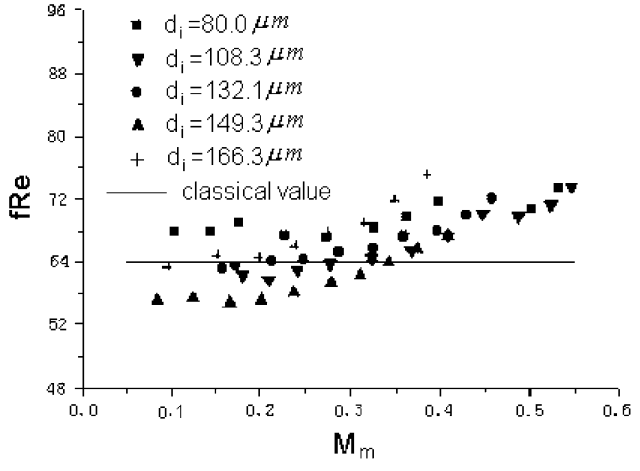

Fig. 10. Frictional factor for gas flow in smooth microtubes (Guo, 2000).

the increase in friction factor is caused by the surface friction induced flow compressibility.

Celata et al. (2000) measured the friction factor for R114 flowing in a channel 130 μm in diameter. The Reynolds number varied from 100 to 8000 and the relative channel surface roughness was 2.65%. Their experimental results show that for laminar flow the friction factor was in good agreement with Hagen–Poiseuille theory for *Re* less than 583. For higher values of *Re*, the experimental data was higher than Hagen–Poiseuille theory. The transition from laminar to turbulent occurred for *Re* in the range of 1881 to 2479, which coincides approximately with the standard value. Wu and Little (1983) estimated the friction factors for gas flow in trapezoidal microchannels with hydraulic diameters ranging from 30 to 60 μm and relative surface roughness between 0.05 and 0.30. Their studies revealed that even for laminar flow the friction factor was influenced by the channel roughness. The experimental values for the friction factor normalized with respect to the theoretical values were found to vary from 1.3 to 3.5. The authors felt that their higher fraction factors were due to the variation of the flow cross-section caused by the large roughness. In addition, the inaccurate measurement of the inner diameter of the tubes may be responsible for such phenomena. Mala and Li (1999) measured the pressure drop and flow rate for the flow of deionized water through tubes with diameters ranging from 50 to 254 μm using stainless steel and fused silicon tubes with mean surface roughnesses between 0.007 and 0.035. Their results indicated significant departure of the flow characteristics for microtubes from the predictions of conventional theory. The theoretical curves for Poiseuille flow fall below the experimental values. As the *Re* increased, the measured pressure gradient was significantly higher than that predicted for Poiseuille flow. The variation of the friction factor, f, with *Re* for microtubes from the data of Mala and Li (1999) is shown in Fig. 11. The variation of f with *Re* for the various kinds of microtubes are similar. As seen from Fig. 11, these curves exhibit three distinct regions. For small *Re*, the friction factor decreases linearly with *Re* on the semi-log plot. For large *Re*, the slope of the curve decreases and approaches zero. Between these two regions, the friction factor follows the transitional curve. The authors accounted for the measured roughness induced momentum transfer by introducing a roughness-viscosity analog to the concept of eddy viscosity in turbulent flow. Mala and Li (1999) concluded that the measured friction was due to an early transition from laminar to turbulent flow and the increased surface roughness effect in microtubes.

Li et al. (2000b) conducted experiments to measure the pressure drop and the flow rate for laminar flow of deionized water through stainless steel microtubes with diameters of 128.8, 136.5 and 179.8 μm and relative

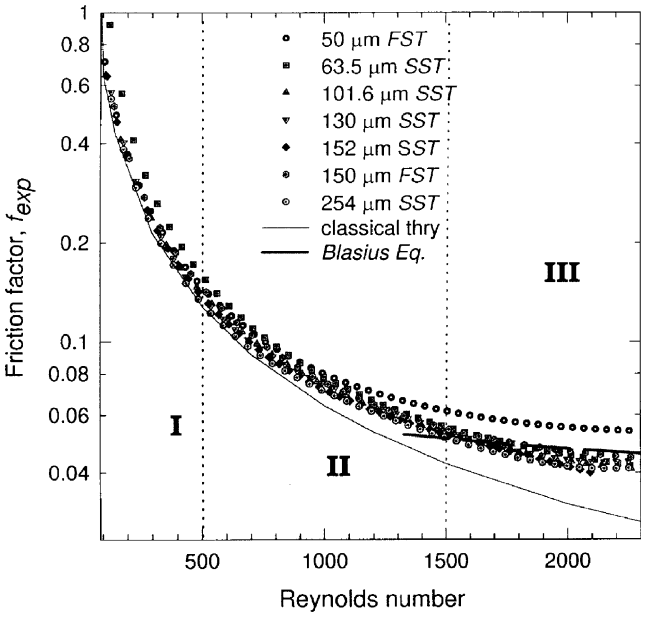

Fig. 11. Friction factor variation for microtubes (Mala and Li, 1999).

surface roughness between 0.03 and 0.043. As shown in Fig. 12, the friction factors for these three cases were 10% to 25% higher than the theoretical values for *Re* between 500 and 2000. The transition from laminar to turbulent flow started at *Re* around 1800.

According to traditional theory, the surface roughness has negligible impact on the friction for laminar flow unless the relative surface roughness is greater than 5%. However, experimental results from Li et al. (2000b), like the results from Mala and Li (1999), indicated that the flow friction in microchannels was higher than the standard value even when the relative roughness was less than 5%.

Du (2000) numerical simulated laminar flow in rough microtubes to study the mechanism for the roughness effect. Based on a scanning electronic microscope (SEM)

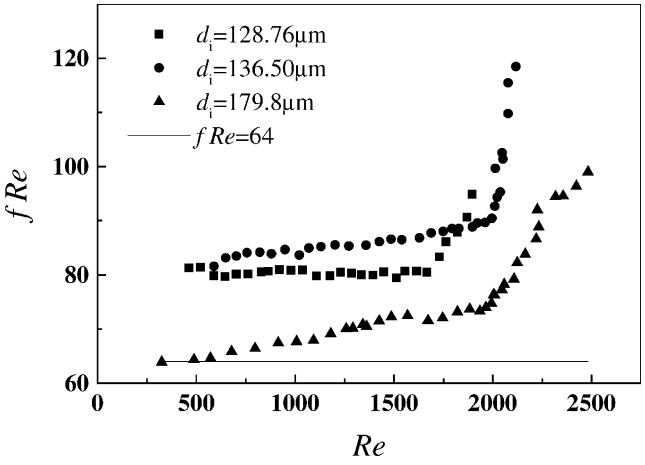

Fig. 12. Friction factor for rough microtubes (Li et al., 2000b).

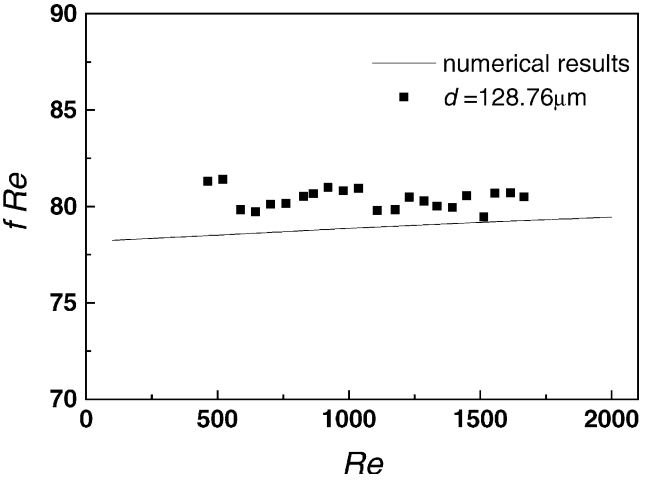

Fig. 13. Comparison of numerical and experimental friction factor results.

photo of the inner surface of a stainless steel microtube, regular three-dimensional roughness elements were used to simulate the surface roughness. The numerical results shown in Fig. 13 were slightly lower than the experimental data. The numerical simulations show that the form drag resulting from the roughness elements is one of the reasons leading to the increased friction factor. Another factor, which may affect the flow in microchannels, is the roughness-generated flow disturbances. For a given relative roughness, the number of roughness elements per unit channel length is much larger for microchannels which would generate more frequent disturbances of the channel flow resulting in an increased friction factor. Finally, such disturbances may cause an early transition from laminar to turbulent flow when *Re* is large enough. In addition, since the turbulence is partly due to the roughness induced disturbances, rather than flow instabilities, the transition from laminar to turbulent might be continuous and smooth.

2.3. Variation of predominate forces

Various kinds of forces simultaneously act on a fluid flowing in a channel. For some flow and heat transfer problems, certain forces are important, while others may be neglected. Since different forces have different length dependences, as listed in Table 1, forces related to surfaces area which are proportional to the length with a lower exponent (for example, the surface tension, the

Table 1
Size effects of forces

Electromagnetic force $\sim L^4$	Inertial force $\sim L^2$
Centrifugal force $\sim L^4$	Viscous force $\sim L^1$
Gravitational force $\sim L^3$	Surface tension $\sim L^1$
Buoyancy $\sim L^3$	Electrostatic force $\sim L^{-2}$

viscous force or the electrostatic force) become more important and even dominant as the scale is reduced.

Recently, Dao et al. (1996) developed a novel accelerometer for various applications. The accelerometer is based on the free convection of a tiny hot air bubble in an enclosed chamber and does not require a solid proof mass, so it is compact, lightweight, and inexpensive to manufacture. Leung et al. (1997) produced the device by bulk-silicon fabrication, and tests with natural gravity demonstrated that its sensitivity could reach 0.6 mg. Milanovic et al. (2000) fabricated two kinds of convective accelerometers, thermopile and thermistor types using standard IC technology. Compared with those proposed by Dao et al. (1996) and by Leung et al. (1997), Milanovic et al. (2000) felt that their accelerometers exhibited some significant advantages, such as low cost, miniaturization, integration and good frequency response. Luo et al. (2001a,b) designed a micromachined convective accelerometer with a structure for a bulk-silicon fabrication based on the performance optimization.

The experimental data showed that the optimized device has better linearity, higher sensitivity and a preferable frequency response than other reported convective accelerometers.

The structure of the micromachined convective accelerometer proposed by Luo et al. (2001a,b) is shown in Fig. 14. It includes a cavity containing air as a working fluid, a heater about 80–100 μm in width and two temperature sensors. Air moves across the sensors by virtue of free convection. The device is packaged in a sealed chamber to prevent outside disturbances. When the electric heater is on, a free convection flow occurs in the cavity.

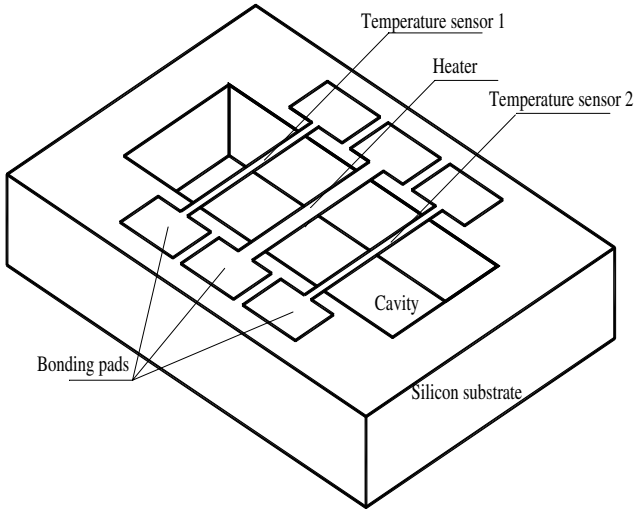

Fig. 14. Micromachined convective accelerometer (Luo et al., 2001a,b).

The temperature profile is symmetrical in the cavity when the accelerometer is not accelerating. There is no temperature difference between the two sensors if they are symmetric relative to the heater and the cavity, and if there is no convection in the axial direction due to acceleration. The acceleration modifies the free convection flow resulting in a skewed temperature field as shown in Fig. 15. The sensor can measure the acceleration since the temperature difference between the two sensors is directly related to the acceleration. For natural convection around conventional-sized object, the buoyancy is largely balanced by the inertial force due to the small contribution of the viscous force. Since the inertial force is of the same order of magnitude as the buoyancy force, then

$$|U \cdot \nabla U| \sim |g\beta\Delta T| \quad \text{and} \quad U \sim (g\beta\Delta T)^{1/2} \tag{5}$$

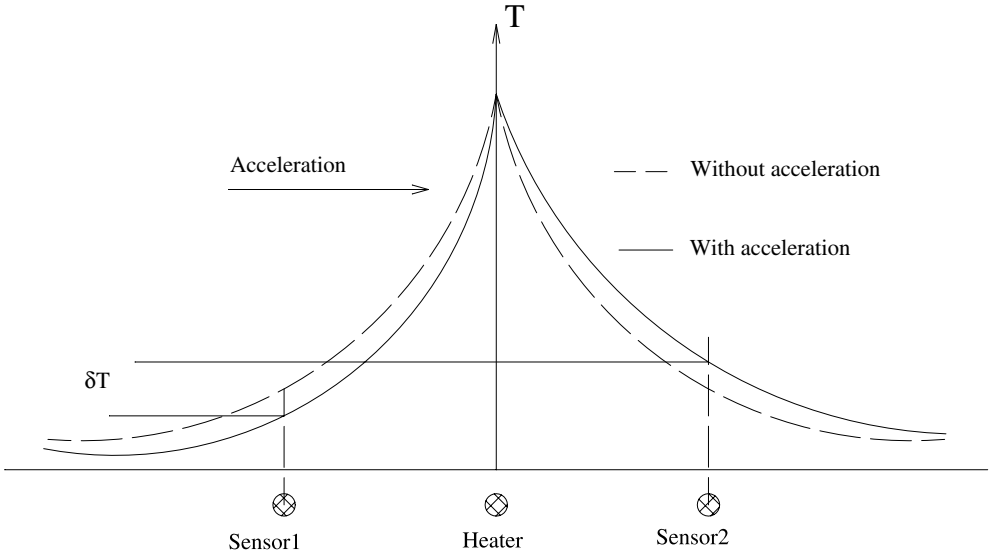

Fig. 15. Temperature distributions in the cavity with/without acceleration.

Therefore, the ratio of the convection to conduction heat transfer is then

$$|U \cdot \nabla T|/|a\nabla^2 T| \sim Ul/a \sim Gr^{1/2}Pr \tag{6}$$

which leads to the well-known heat transfer correlation, $Nu \sim Gr^{1/4}$.

As the object size decreases, the viscous force dominates the inertial force at small Grashof numbers, the viscous force largely balances the buoyancy force,

$$|v\nabla^2 U| \sim |g\beta\Delta T| \quad \text{and} \quad U \sim g\beta\Delta T l^3/v \tag{7}$$

Therefore, the ratio of the convection to conduction heat transfer is then proportional to Gr as follows:

$$|U \cdot \nabla T|/|a\nabla^2 T| \sim Ul/a \sim GrPr \tag{8}$$

As a result, the heat transfer correlation must differ from that for natural convection on at large scale. The numerical results for natural convection on a two-dimensional vertical plate with Gr ranging from 10^0 to 10^8 are given in Fig. 16. It can be found that he buoyancy is mainly balanced by the inertial force for Gr from 10^6 to 10^8, while the inertial force can be neglected for Gr from 10^1 to 10^4. This is why $Nu \sim Gr^{1/4}$ for Gr from 10^6 to 10^8, while, there must be a different correlation between Nu and Gr for Gr from 10^1 to 10^4.

Luo et al. (2001a,b) numerically studied the relative importance of the various forces for natural convection in a square cavity as shown in Fig. 17. The top and the bottom surfaces were adiabatic. The left and right surface temperatures were 303 and 293 K. The numerical simulation used a laminar flow model due to the small Rayleigh number. The numerical results on the relative contribution of the various forces in the region near the hot wall, $x/L = 0.02$, are shown in Fig. 17 for Rayleigh number ranging from 10^2 to 10^9, where ε is defined as the ratio of the inertial force to the viscous force.

The contribution of the inertial force to the natural convection is much less than that of the viscous force for

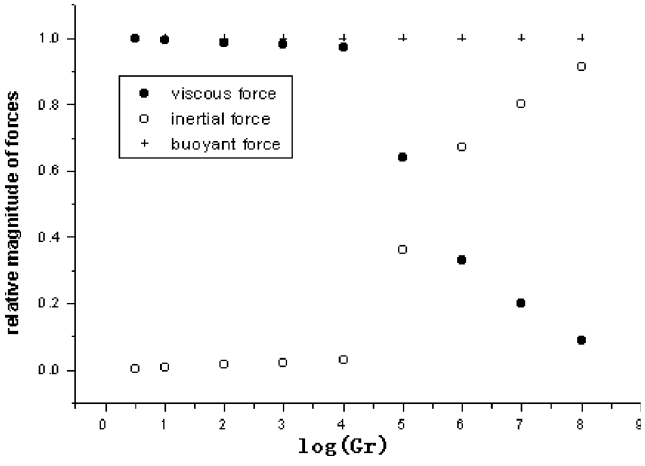

Fig. 16. Relative importance of inertial and viscous forces for natural convection on a two-dimensional vertical plate (Guo, 2000).

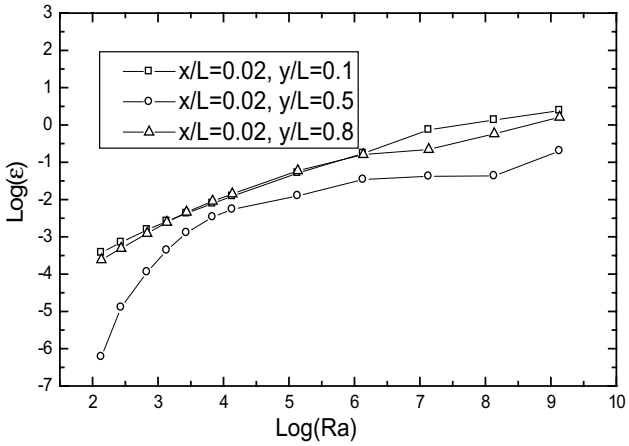

Fig. 17. Ratio of the inertial to viscous forces for flow in a square cavity.

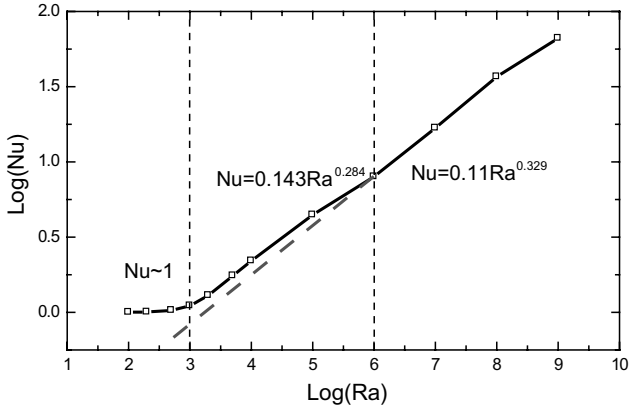

Fig. 18. Ratio of the inertial to viscous forces for flow in a square cavity (Luo et al., 2001a,b).

Rayleigh numbers less than 10^6. The variation of the dominant forces for the different Rayleigh number regimes will result in different relationships between the Nusselt number and the Rayleigh number as plotted in Fig. 18. The heat transfer due to natural convection can be divided into three regions. For $Ra > 10^6$, it is well known that $Nu \sim Ra^{0.33}$. For natural convection in a microenclosure with Ra ranging from 10^3 to 10^6, the inertial force is negligible, so $Nu \sim Ra^{0.284}$. If $Ra < 10^3$, the natural convection decrease towards zero so the heat transfer is only due to heat conduction as both the viscous and inertial forces can be neglected. It is worthy noting that the heat transfer may be underestimated if conventional heat transfer correlations are used for microscale natural convection, as indicated in Fig. 18 (see the dash line).

2.4. Axial heat conduction in the channel wall

Mori et al. (1974) and Shah and London (1978) studied the effect of axial heat conduction in the wall on

the convection heat transfer and found that the Nusselt number must fall in between 4.36 and 3.66, which correspond to Nusselt numbers for constant heat flux and constant temperature boundary conditions respectively. In order to quantitatively describe the effect of the axial heat conduction in the wall on convection heat transfer a conductance number was given by Chiou (1980)

$$\text{cond} = \frac{k_s A_s}{L\dot{m}_f c_{p,f}} = \frac{A_s/A_f}{L/D}\frac{1}{RePr}\frac{k_s}{k_f} \tag{9}$$

where k_s, A_s, k_f, A_f are the thermal conductivity and cross-sectional area for tube wall and fluid, L, tube length, D, tube diameter, $\dot{m}_f$, the fluid mass flow rate, and $c_{p,f}$, the specific heat of the fluid. He indicated that the effect of axial heat conduction in the channel wall on the convective heat transfer can be ignored, if the conductance number is less than 0.005. It is obvious that the effect of the axial heat conduction depends on the ratio of the wall to fluid thermal conductivity and the ratio of channel wall thickness to diameter, as well as Peclet number. The ratio of the channel wall thickness to diameter for a fixed wall thickness, which corresponds the surface to volume ratio, increases with reducing the channel diameter. Hence, the axial heat conduction in the channel wall for conventional-size channels can usually be neglected because the wall thickness is very small compared to the channel diameter, while for flow in microchannels, the wall thickness can be of the same order or larger than the channel diameter, which will affect the flow and heat transfer in the microchannels.

Some existing experimental results for heat transfer in microchannels differ significantly from that for conventional-size channels. For example, Choi et al. (1991) reported that the average Nusselt numbers in microchannels with hydraulic diameters from 9.7 to 81.2 μm were much lower than that for standard channels and increased with increasing Reynolds number as shown in Fig. 19. Takano (2001) obtained similar results for heat transfer in a circular microtube with an inner diameter of 52.9 μm and an outer diameter of 144.7 μm, as also shown in Fig. 19, although his experimental results in friction factor coincide with classical value. Both they applied one-dimensional assumption to estimate the overall thermal resistance from the fluid outside to the fluid inside the channel as follows:

$$\frac{1}{U} = \frac{1}{h_i 2\pi r_i} + \frac{1}{2\pi k_s}\ln\left(\frac{r_o}{r_i}\right) + \frac{1}{h_o 2\pi r_o} \tag{10a}$$

$$U = -\frac{\rho c_p u_m \pi r_i^2}{L}\ln\left(\frac{T_2 - T_{0,\infty}}{T_1 - T_{0,\infty}}\right) \tag{10b}$$

$$Nu = -\frac{k^* RePr \ln\theta_2}{2L^* k^* + RePr\ln\theta_2\left(\ln D^* + \frac{1}{Bi_o}\right)} \tag{10c}$$

where h_i, h_o are the inner and outer heat transfer coefficients, U, the overall heat transfer coefficient, r_i, r_o, the inner and outer radius, k_s, the thermal conductivity of the tube wall, ρ, fluid density, c_p, heat capacity of the fluid, u_m, the mean fluid velocity, T_1, T_2, the fluid temperatures at inlet and outlet, and the non-dimensional parameters are defined as, $k^* = k_s/k_f$, $L^* = L/D_i$, $D^* = D_o/D_i$, $\theta_2 = (T_2 - T_{0,\infty})/(T_1 - T_{0,\infty})$.

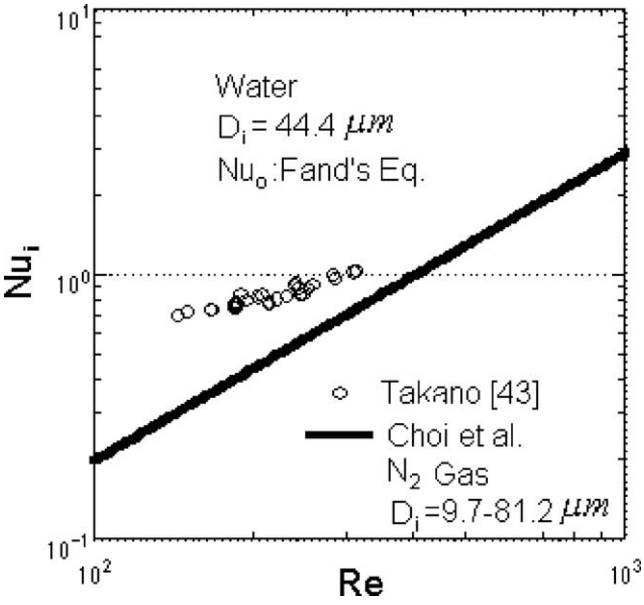

Fig. 19. Nusselt number variation for microchannels (Takano, 2001).

We try to know the reason why for the fully developed smooth tube flow the Nusselt numbers obtained by Choi et al. (1991) and Takano (2001) in terms of experiment are dependent on Reynolds number and much lower than the standard value. To exam whether the axial heat conduction should be responsible for such an unusual phenomenon, numerical solution of the governing equations of the conjugated heat transfer problems with third kind of boundary condition (as shown in Fig. 20) was carried out to investigate the effect of the axial heat conduction on Nusselt number. Some of numerical results are demonstrated in Figs. 21 and 22. It can be found in Fig. 21 that the larger conductivity ratio (higher wall conductivity) leads to the lower Nusselt number, whose value approaches to that for the tube flow with constant wall temperature boundary condition. On the contrary, Nusselt number is close to that for the tube flow with constant heat flux boundary condition, if the wall conductivity is very low (very small conductivity ratio) and the axial heat conduction in the wall may be neglected in this case. The wall thickness effect is given in Fig. 22. The Nusselt number for the fully developed channel flow decreases with decreasing the diameter ratio. These results show that the axial heat conduction in the tube wall will affect the value of Nusselt number, but will not make Nusselt number much lower than their standard values.

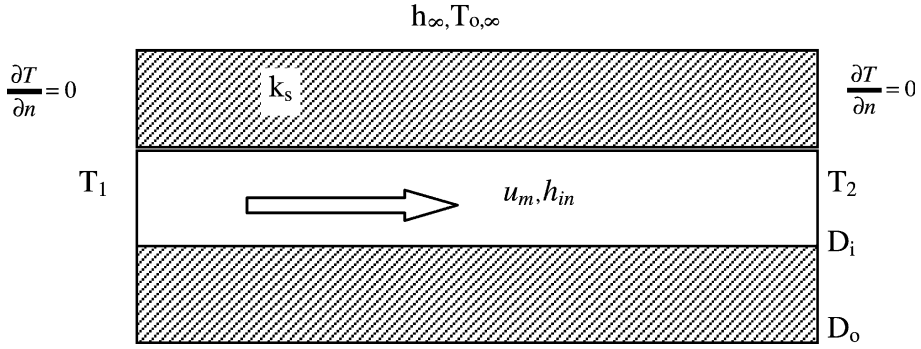

Fig. 20. Schematic of the tube flow.

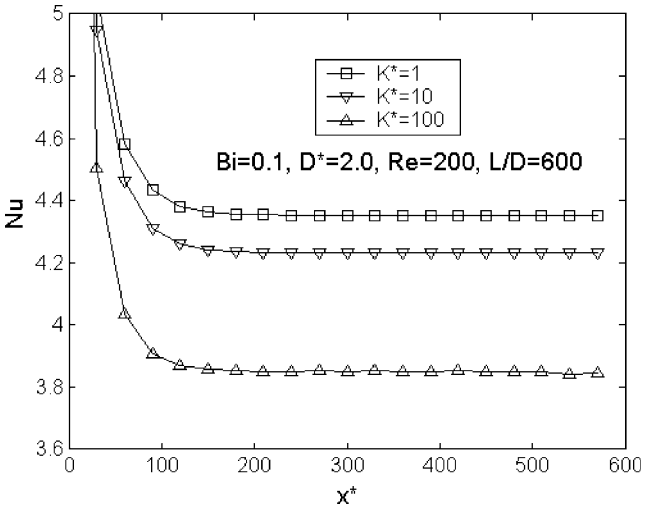

Fig. 21. Effect of thermal conductivity ratio on Nusselt number.

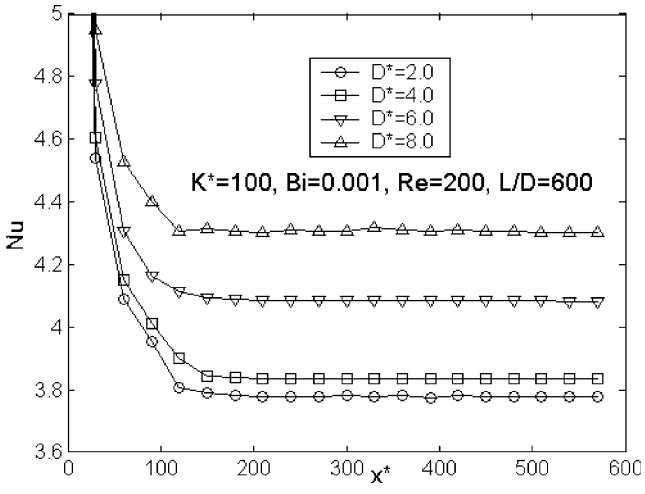

Fig. 22. Effect of diameter ratio on the Nusselt number.

Therefore, it is necessary to exam the applicability of one-dimensional model of thermal resistance which is usually adopted in the data processing because 1-D model is based on the assumption of no axial heat conduction in the wall. For this purpose Nusselt number has been calculated in terms of Eq. (10), where T_1, T_2 and $T_{0,\infty}$, k_s, D, Re are regarded as known parameters because they are measurable in experiments. Calculated results in Nusselt number are given in Figs. 23 and 24,

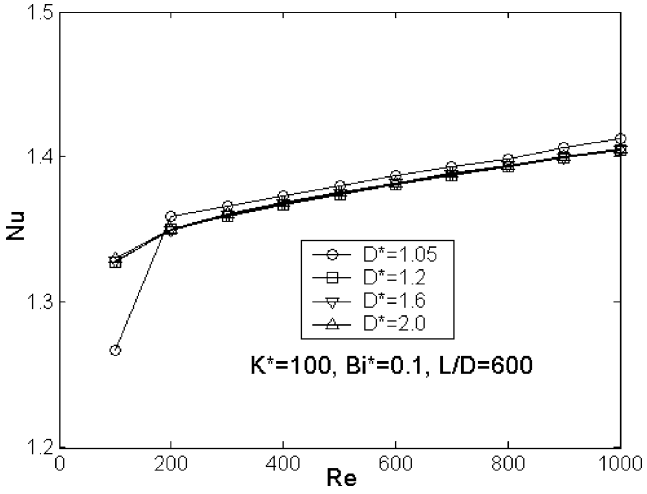

Fig. 23. Nusselt number versus Reynolds number with diameter ratio (1-D model) as parameter.

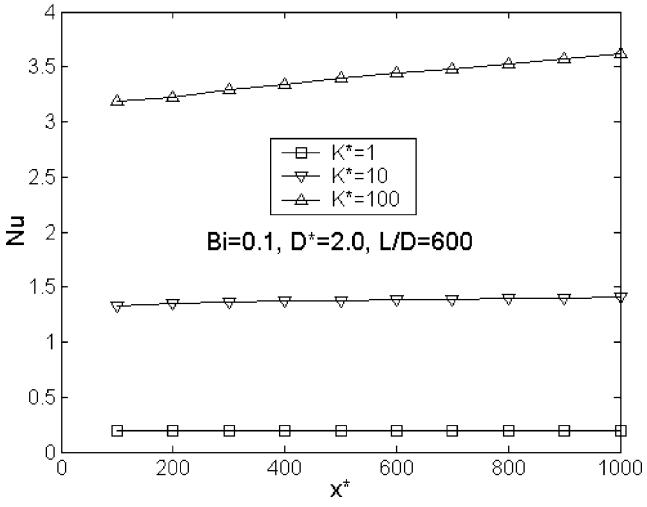

Fig. 24. Nusselt number versus Reynolds number with conductivity ratio (1-D model) as parameter.

which have similar trend with the experimental results reported by Choi et al. (1991) and Takano (2001), that is, Nusselt numbers are lower than the conventional one and decrease with decreasing Reynolds numbers. This indicates that the deviation of Nusselt numbers is caused by use of the one-dimensional thermal resistance model based on the assumption without axial heat conduction in the channel wall. Furthermore, such a deviation induced by the axial heat conduction increases with decreasing the Reynolds numbers and increasing the diameter ratio or thermal conductivity ratio.

3. Variation of other predominant factors

3.1. Effect of surface geometry

The hydraulic diameter is commonly used to characterize the flow and heat transfer in non-circular conventional-sized tubes. For liquid flow in microchannels, dissolved gases in the liquid or gases absorbed on the surface may have considerable impact on the flow and heat transfer characteristics. As such gases collect in the corners of non-circular channels, the wetted perimeter will be reduced and the fluid velocity will increase as the actual flow cross-section is reduced. The smaller perimeter reduces the friction while the large velocity increases the friction. Square and equilateral triangle channels were analyzed numerically as examples.

The geometry and size of gas bubbles in the channel corners are dependent on the liquid surface tension and contact angle. The results for square and triangular microchannels are given in Fig. 25, where a is the length of the microchannel side and θ and r describe the gas volume as shown. The numerical results describe the variation of the wetted perimeter and the mean velocity with the angle, θ, which is related to the gas bubble size,

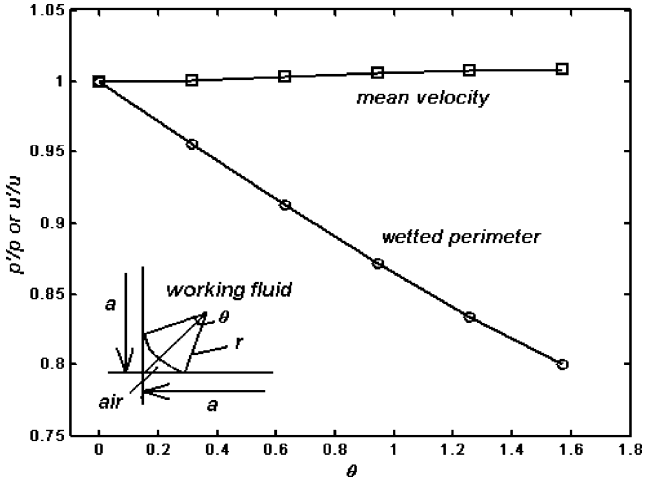

Fig. 25. Variations of mean velocity and wetted perimeter with contact angle for a square channel.

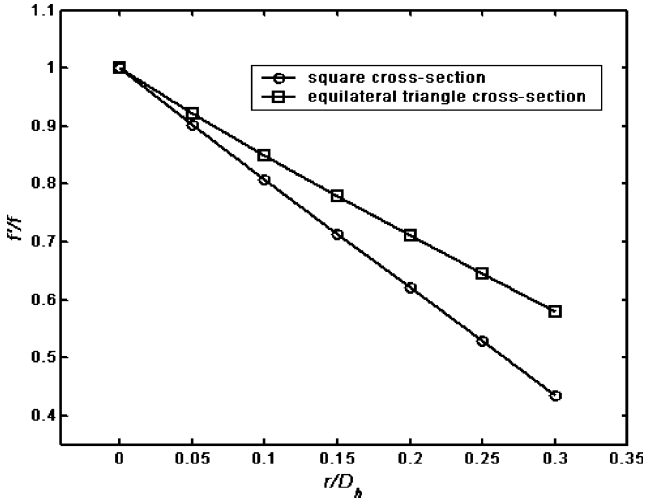

Fig. 26. Friction factors for liquid flows in square and equilateral triangle channels.

where u' and p' represent the mean velocity and the wetted perimeter. The results in Fig. 25 show that the wetted perimeter is more strongly dependent on the bubble size than the mean velocity. Therefore, the friction decrease due to the reduced wetted perimeter will be larger than the friction increase due to the increased mean velocity. The dependence of the normalized friction factor on the ratio of r/D_h is illustrated for microchannels with square and equilateral triangle cross-sections in Fig. 26, where r and D_h are the arc radius and channel hydraulic diameter. This dependence will differ for channels with different surface geometries. In experiments, the gases on the surface or dissolved gases come out of solution will reduce the measured friction factor relative to standard values. The larger the ratio of the channel surface area to volume is, the larger the discrepancies is between experimental results and standard values for the friction factor. It means that the smaller or non-circular channel will then have larger discrepancies between experimental results and the conventional ones. Hence, the use of the hydraulic diameter is problematic for comparing correlations for liquid flow in microchannels with different geometries and for the same geometry with different sizes.

3.2. Effect of measurement accuracy

In the experiments of flow and heat transfer in microchannels, some parameters, such as the flow rate and channel dimensions are difficult to measure accurately because they are very small. For example, the relative error of the measured channel height reported by Pfahler et al. (1990b) was up to 20%.

In our experiments measuring the flow resistance in a circular glass microtube, we initially measured the diameter as 84.7 μm using a 40× microscope. The data

reduction with this measured diameter showed that the friction factors were larger than that predicted by conventional theory. The average value of the diameter measured using a 400× microscope and a SEM for the same microtube was only 80.0 μm. With this more accurate value of the diameter, the frictional factors obtained from the experimental data were in good agreement with the conventional values.

For single-phase flow in microchannels, Palm (2001) suggested that some of the deviations in the experimental results may be caused by the difficulties in accurately determining the hydraulic diameters. Du et al. (2000) carried out an uncertainty analysis of the Darcy equation for incompressible flow in circular channel flows. The uncertainty of fRe is

$$\frac{\delta(fRe)}{(fRe)} = \left\{ \left(\frac{\delta(\Delta p)}{\Delta p} \right)^2 + \left(4\frac{\delta d}{d} \right)^2 + \left(-\frac{\delta l}{l} \right)^2 + \left(-\frac{\delta m}{m} \right)^2 \right\}^{1/2} \quad (11)$$

where m, Δp, d, l are the mass flow rate, pressure drop, tube diameter and tube length. Eq. (11) shows that the tube diameter measurement error may play a very important part in the uncertainty of the friction factor, fRe. The discrepancies among different friction factor and heat transfer correlations proposed by various investigators may be, at least in part, attributed to the uncertainties of the experimental data.

4. Concluding remarks

(1) The physical mechanisms for the size effect on the microchannel flow and heat transfer can be divided into two classifications: (a) The gas rarefaction effect occurs when the continuum assumption breaks down as the characteristic length of the flow becomes comparable to the mean free path of the molecules. (b) Variations of the predominant factors influence the relative importance of various phenomena on the flow and heat transfer as the characteristic length decreases, even if the continuum assumption is still valid.

(2) Since the characteristic lengths of flows in MEMS are from 1 μm ($Kn \sim 0.1$) to fractions of 1 mm ($Kn \sim 0.0001$), in most cases the assumption of flow continuum is usually valid. Hence, the size effect on the flow and heat transfer should be largely attributed to the variation of the predominant factors or phenomena in the flow and heat transfer processes.

(3) The large surface area to volume ratio should be responsible for the size effects on flow and heat transfer in microchannel with diameter larger than one micrometer ($Kn < 0.1$); As the surface to volume ratio is very large for microchannel flow, factors which are related to the surface area become more important and even dominant over factors related to the volume effect. Among these are: (a) surface friction induced flow compressibility, which makes the fluid velocity profiles flatter and leads to higher friction factors and Nusselt numbers; (b) surface roughness, which is likely responsible for the early transition from laminar to turbulent flow and the increased friction factor and Nusselt number; (c) the importance of surface related viscous force in natural convection, which modifies the correlation between Nu and Ra for natural convection in a microenclosure; and (d) other surface related effects, which include the axial heat conduction in the channel wall channel and the surface geometry. All these factors may cause the flow and heat transfer behavior in microchannels differ from that at conventional scales.

(4) Discrepancies between experimental results for the friction factor and the Nusselt number and their standard values due to the measurement errors or entrance region effects might be misunderstood as being caused by novel phenomena at microscales. For instance, there is no reason for the early transition from laminar to turbulent flow in the absence of any special effects.

Acknowledgement

This paper was financially supported by the National Natural Science Foundation of China with Grant number 59995550-2.

References

Beskok, A., George, E.K., William, T., 1996. Rarefaction and compressibility effects in gas microflows. ASME J. Fluid Eng. 118, 448–456.

Celata, G.P., Cumo, M., Gulielmi, M., Zummo, G., 2000. Experimental investigation of hydraulic and single phase heat transfer in 0.130 mm capillary tube. In: Celata, G.P. et al. (Eds.), Proceedings of the International Conference on Heat Transfer and Transport Phenomena in Microscale. Begell House, Inc., New York, pp. 108–113.

Chiou, J.P., 1980. The advancement of compact heat exchanger theory considering the effects of longitudinal heat conduction and flow nonuniformity. In: Shah, R.K., McDonald, C.F., Howard, C.P. (Eds.), Symposium on Compact Heat Exchangers—History, Technological Advancement and Mechanical Design Problems. In: HTD, vol. 10. ASME, New York, pp. 101–121, Book No. G00183.

Choi, S.B., Barron, R.F., Warrington, R.Q., 1991. Fluid flow and heat transfer in micro tubes. ASME DSC-32, 123–133.

Dao, R., Morgan, D.E., Kries, H.H., Bachelder, D.M., 1996. Convective accelerometer and inclinometer. United States Patent 5581034.

Drain, K. et al., 1995. Single phase forced convection heat transfer in microgeometries—a review. In: Proceedings of 30th Intersociety Energy Conversion Engineering Conference, Florida, 1995.

Drew, T.B., Koo, E.C., McAdams, W.H., 1932. The friction factor for clean round pipes. Trans. AIChE 28, 56–72.

Du, D.X., 2000. Effect of compressibility and roughness on flow and heat transfer in microtubes. Doctoral degree thesis, Tsinghua University, 2000.

Du, D.X., Li, Z.X., Guo, Z.Y., 2000. Friction resistance for gas flow in smooth microtubes. Sci. Chi. (Ser. E) 43 (2), 171–177.

Gad-ed-Hak, M., 1999. The fluid mechanics of microdevices—the Freeman scholar lecture. J. Fluid Eng. 121, 5–33.

Guo, Z.Y., 2000. Characteristics of microscale fluid flow and heat transfer I MEMS. In: Proceedings of the International conference on Heat Transfer and Transport Phenomena in Microscale, Banff, Canada, 2000. pp. 24–31.

Guo, Z.Y., Wu, X.B., 1997. Compressibility effect on the gas flow and heat transfer in a micro tube. Int. J. Heat Mass Transfer 40, 3251–3254.

Guo, Z.Y., Wu, X.B., 1998. Further study on compressibility effect on the gas flow and heat transfer in a microtube. Microscale Thermophys. Eng. 2, 111–120.

Harley, J., Huang, Y., Bau, H., Zemel, J., 1995. Gas flow in microchannel. J. Fluid Mech. 284, 257–274.

Jerman, J.H., 1990. Electrically-activated, micromachined diaphragm valves. In: IEEE Solid-State Sensor and Actuator Workshop, June 4–7, 1990. IEEE, pp. 65–69., Sponsored by: IEEE Electron Devices Soc.

Johan, K. et al., 2001. Liquid transport properties in sub-micron channel flows. In: Proceedings of 2001 ASME International Mechanical Congress and Exposition, New York, NY, November 11–16, 2001.

Karniadakis, G.E., Beskok, A., 2002. Micro Flows. Springer-Verlag Inc., New York.

Kemler, E., 1933. A study of the data on the flow of fluids in pipes. Trans. ASME 55, 7–32, paper Hyd-55-2.

Leung, A.M., Jones, J., Czyzewska, E., Chen, J., Pascal, M., 1997. Micromachined accelerometer with no proof mass, Technical Digest of Int. Electron Device Meeting, pp. 899–902.

Li, Z.X., Xia, Z.Z., Du, D.X., 1999. Analytical and experimental investigation on gas flow in a microtube. In: Kyoto University–Tsinghua University Joint Conference on Energy and Environment, Kyoto, Japan, November 1999. pp. 1–6.

Li, Z.X., Du, D.X., Guo, Z.Y., 2000. Investigation on the characteristics of frictional resistance of gas flow in microtubes. In: Proceedings of Symposium on Energy Engineering in the 21st Century, 2000, vol. 2. pp. 658–664.

Li, Z.X., Du, D.X., Guo, Z.Y., 2000. Experimental study on flow characteristics of liquid in circular microtubes. In: Proceedings of the International conference on Heat Transfer and Transport Phenomena in Microscale, Banff, Canada, 2000. pp. 162–167.

Luo, X.B., Yang, Y.J., Zhang, Z., Li, Z.X., Guo, Z.Y., 2001a. An optimized micromachined convective accelerometer with no proof mass. J. Micromech. Microeng. 11, 504–508.

Luo, X.B., Li, Z.X., Guo, Z.Y., 2001b. Effect of size variation on laminar natural convection in a square cavity. In: Proceedings of 10th Annual Conference of Engineering Thermophysics Society of China, 2000. Heat and Mass Transfer, vol. 1. pp. 122–125.

Mala, G.M., Li, D., 1999. Flow characteristics of water in microtubes. Int. J. Heat Fluid Flow 20, 142–148.

Mehendale, S.S., Jacobi, A.M., Shah, R.K., 1999. Heat exchangers at micro- and meso-scales. In: Proceedings of the International Conference on Compact Heat Exchangers and Enhance Technology for the Process Industries, Banff, Canada, 1999. pp. 55–74.

Milanovic, V., Bowen, E., Zaghloul, M.E., et al., 2000. Micromachined convective accelerometers in standard integrated circuits technology. Appl. Phys. Lett. 76 (4), 508–510.

Moody, L.F., 1944. Friction factors for pipe flow. Trans. ASME 66, 671–684.

Mori, S., Sakakibara, M., Tanimoto, A., 1974. Steady heat transfer to laminar flow in a circular tube with conduction in tube wall. Heat Transfer—Jpn. Res. 3 (2), 37–46.

Nikuradse, J., 1933. Strmungsgesetze in rauhen rohren. V.D.I. Forschungsheft 361, 1–22.

Palm, R., 2001. Heat transfer in microchannels. Microscale Thermophys. Eng. 5 (3), 155–175.

Papautsky, I., Brazzle, J., Ameel, T., Frazier, A.B., 1999a. Laminar fluid behavior in microchannels using micropolar fluid theory. Sens. Actuators 73, 101–108.

Papautsky, I., Gale, B., Mohanty, K.S., Ameel, T.A., Frazier, A.B., 1999. Effects of rectangular microchannel aspect ratio on laminar friction constant. In: Proceedings of SPIE, Microfluidic Devices and Systems II, 1999, vol. 3877. pp. 147–158.

Pfahler, J., Harley, J., Bau, H., 1990a. Liquid and gas transport in small channels. ASME DSC-19, 149–157.

Pfahler, J., Harley, J., Bau, H., 1990b. Liquid transport in micron and submicron channels. Sens. Actuators A21–A23, 431–434.

Pfahler, J., Harley, J., Bau, H., 1991. Gas and liquid flow in small channels. ASME DSC-32, 49–60.

Pigott, R.J.S, 1933. The flow of fluids in closed conduits. Mech. Eng. 55, 497–501, 515.

Shah, R.K., London, A.L., 1978. Laminar flow forced convection in ducts. In: Irvine, T.F., Hartnett, J.P. (Eds.), Advances in Heat Transfer (Suppl. 1). Academic Press, New York, San Francisco, London.

Takano, K., 2001. Personal correspondence, June 19, 2001.

van der Berg, R.H., Seldam, C.A., ven der Gulik, P.S., 1993a. Compressible laminar flow in a capillary. J. Fluid Mech. 246, 1020.

van der Berg, R.H., Seldam, C.A., ven der Gulik, P.S., 1993b. Thermal effects in compressible viscous flow in a capillary. Int. J. Thermophys. 14, 865–892.

Wang, B.X., Peng, X.F., 1994. Experimental investigation of liquid forced-convection heat transfer through microchannels. Int. J. Heat Mass Transfer 37, 73–82.

Webb, R.L., Zhang, M., 1998. Heat transfer and friction in small diameter channels. Microscale Thermophys. Eng. 2, 189–202.

Wu, P.Y., Little, W.A., 1983. Measurement of friction factors for the flow of gases in very fine channels used for microminiature Joule–Thomson refrigerators. Cryogenics 23, 273–277.

Wu, P.Y., Little, W.A., 1984. Measurement of the heat transfer characteristics of gas flow in fine channel heat exchangers used for microminiature refrigerators. Cryogenics 24, 415–420.